Environmental Science & Technology

pubs.acs.org/est

Article

Variability and Time of Day Dependence of Ozone Photochemistry in Western Wildfire Plumes

Michael A. Robinson, Zachary C. J. Decker, Kelley C. Barsanti, Matthew M. Coggon, Frank M. Flocke, Alessandro Franchin, Carley D. Fredrickson, Jessica B. Gilman, Georgios I. Gkatzelis, Christopher D. Holmes, Aaron Lamplugh, Avi Lavi, Ann M. Middlebrook, Denise M. Montzka, Brett B. Palm, Jeff Peischl, Brad Pierce, Rebecca H. Schwantes, Kanako Sekimoto, Vanessa Selimovic, Geoffrey S. Tyndall, Joel A. Thornton, Paul Van Rooy, Carsten Warneke, Andrew J. Weinheimer, and Steven S. Brown*

Cite This: https://doi.org/10.1021/acs.est.1c01963

Read Online

ACCESS | Metrics & More | Article Recommendations | Supporting Information

ABSTRACT: Understanding the efficiency and variability of photochemical ozone (O_3) production from western wildfire plumes is important to accurately estimate their influence on North American air quality. A set of photochemical measurements were made from the NOAA Twin Otter research aircraft as a part of the Fire Influence on Regional to Global Environments and Air Quality (FIREX-AQ) experiment. We use a zero-dimensional (0-D) box model to investigate the chemistry driving O_3 production in modeled plumes. Modeled afternoon plumes reached a maximum O_3 mixing ratio of 140 ± 50 ppbv (average ± standard deviation) within 20 ± 10 min of emission compared to 76 ± 12 ppbv in 60 ± 30 min in evening plumes. Afternoon and evening maximum O_3 isopleths indicate that plumes were near their peak in NO_x efficiency. A radical budget describes the NO_x volatile - organic compound (VOC) sensitivities of these plumes. Afternoon plumes displayed a rapid transition from VOC-sensitive to NO_x-sensitive chemistry, driven by HO_x (=OH + HO_2) production from photolysis of nitrous acid (HONO) (48 ± 20% of primary HO_x) and formaldehyde (HCHO) (26 ± 9%) emitted directly from the fire. Evening plumes exhibit a slower transition from peak NO_x efficiency to VOC-sensitive O_3 production caused by a reduction in photolysis rates and fire emissions. HO_x production in evening plumes is controlled by HONO photolysis (53 ± 7%), HCHO photolysis (18 ± 9%), and alkene ozonolysis (17 ± 9%).

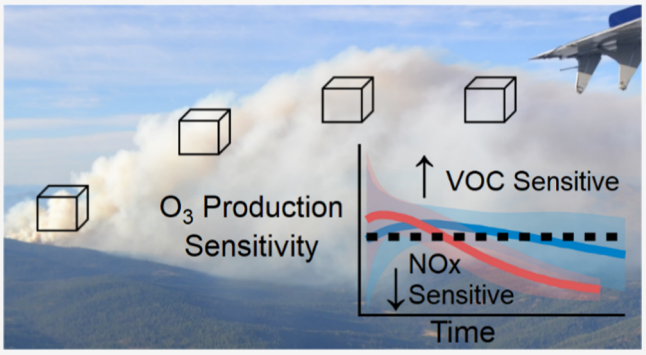

KEYWORDS: *oxidation, volatile organic compounds, biomass, photodissociation, atmospheric chemistry*

1. INTRODUCTION

Emissions from wildfires have significant and increasing impacts on local and regional air quality in the western United States (U.S.). Pollutants such as $PM_{2.5}$ (particulate matter <2.5 μm aerodynamic diameter) and ozone (O_3) regularly exceed U.S. National Ambient Air Quality Standards in the western U.S. nearly every fire season.[1−7] Ozone is a secondary pollutant, formed in the troposphere by the oxidation of volatile organic compounds (VOCs) in the presence of nitrogen oxides (NO_x = NO + NO_2) and sunlight.[8,9] While biomass burning (BB), including wildfires, is estimated to contribute only 3.4% to total NO_x emissions in the United States,[10,11] NO_x emissions from fossil fuels have steadily declined, decreasing by 65% from 1990 to 2019.[11] Concurrently, western U.S. wildfire emissions have been increasing for two decades due to growing frequency and intensity of fires.[12−14] These trends are likely to continue due to decreasing snowpack, increasing summertime temperatures, drought, and human-caused ignitions.[15,16]

Biomass burning emissions are rich in O_3 precursors,[17−19] including VOCs, reactive nitrogen compounds, and photolytic radical sources. Reactive nitrogen in BB plumes includes NO_x and nitrous acid (HONO), the latter also being an important radical source.[20] Plumes from BB emit large amounts of highly reactive VOCs, including small oxygenates (e.g., formaldehyde, acetaldehyde), alkenes (e.g., ethene, propene, butene, 1,3-butadiene), aromatics (e.g., catechol, phenol, benzene, and

Received: March 25, 2021
Revised: June 26, 2021
Accepted: June 28, 2021

Downloaded via US EPA OFFICE OF ENVIRONMENTAL INFO on July 14, 2021 at 14:53:23 (UTC).
See https://pubs.acs.org/sharingguidelines for options on how to legitimately share published articles.

© XXXX American Chemical Society

Table 1. NOAA Twin Otter Measurements Used in This Work

measurement	method	sample frequency	uncertainty (2σ)	reference
NO, NO_2, O_3	chemiluminescence	1 Hz	NO: ±38%, NO_2: ±21%, O_3: ±5%	Sparks et al.[47] Juncosa Calahorrano et al.[48]
CO, CO_2, CH_4, H_2O	cavity ring down spectroscopy	0.5 Hz	CO_2: ±0.200 ppmv, CO: ±0.030 ppmv, CH_4: ±0.002 ppmv, H_2O: ±0.150%	Crosson[49]
BBVOCs[a]	2-D gas chromatography−mass spectrometry	5 min	±30%	Mondello et al.[50] Hatch et al.[51]
HNO_2, C_6H_6O, $C_6H_6O_2$, C_7H_8O, $C_5H_9NO_4$[b]	iodide-adduct chemical ionization mass spectrometry (I^- CIMS)	2 Hz	±30%	Lee et al.[52] Palm et al.[53] Peng et al.[46]
pNO_3, $pC_6H_5NO_4$[c]	aerosol mass spectrometry (AMS)	1 Hz	±30%	DeCarlo et al.[54] Liggio et al.[55] Fry et al.[56]
jNO_2	filter radiometer	1 Hz	±10%	Warneke et al.[57]

[a]Furan, methyl vinyl ketone, methyl ethyl ketone, α-pinene, β-pinene, limonene (see Figures S5 and S6). [b]Assumed structures, nitrous acid (HONO), phenol, catechol, cresol, isoprene hydroxy nitrates. [c]Particulate nitrate (pNO_3) and particulate nitrocatechol ion marker ($pC_6H_5NO_4^+$) (see Figure S8).

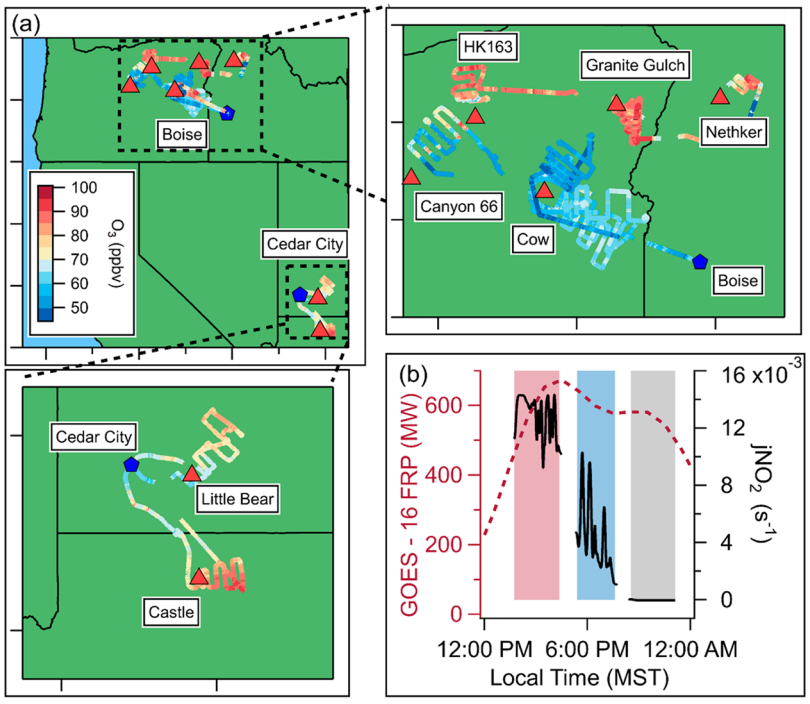

Figure 1. (a) Map of sampled fire complexes during FIREX-AQ, colored by O_3 mixing ratio. (b) Time series of jNO_2 (black trace) measured by the NOAA Twin Otter during a typical flight day (8/28/2019) and measured GOES-16 fire radiative power (FRP) for the Cow 4 fire (red dashed trace). Peak actinic flux (jNO_2) and FRP occur during the afternoon sampling window (shaded in red). Evening plume sampling (shaded in blue) demonstrates a sharp decrease in actinic flux and a moderate decrease in FRP.

toluene), furans (e.g., furan, 2-furfural, furanone), and terpenes (e.g., isoprene, monoterpenes, oxygenated monoterpenes, and sesquiterpenes).[21−25] Several of these VOC classes are also photochemical radical sources, including formaldehyde (HCHO), glyoxal, and other aldehydes.

The relationships between O_3 and its major precursors (NO_x, VOCs, and radical sources) follow well-known, nonlinear functions.[9,26−29] The relationship between O_3 and NO_x is linear at low NO_x mixing ratios (NO_x-sensitive regime) but decreases with increasing NO_x mixing ratios (VOC-sensitive regime). The NO_x sensitivity of O_3 production can be defined by the relative amount of VOCs and radical precursors.[27,30] The NO_x−VOC−radical system, while well studied for urban areas, has received less attention in wildfire plumes, which are chemically complex. Recent laboratory studies and aircraft-based field campaigns have better defined BB emissions[21,22,24,31,32] by characterizing BBVOCs and major radical sources, which both differ from the urban case.[33−38] Understanding the NO_x−VOC−radical sensitivity in BB plumes serves to better define their downwind impacts on air quality.

Analysis of aircraft observations of O_3 photochemistry in BB plumes remains limited despite an increasing number of recent investigations. A box modeling analysis during the 1992

https://doi.org/10.1021/acs.est.1c01963
Environ. Sci. Technol. XXXX, XXX, XXX−XXX

SAFARI campaign emphasized the importance of properly parameterizing dilution with a conserved tracer (e.g., carbon monoxide (CO)).[39,40] Further, the 2000 SAFARI campaign in Otavia, Namibia, modeled O_3 production in young savanna BB plumes.[41−43] These savanna BB plumes displayed NO_x-sensitive O_3 photochemistry controlled by HCHO photolysis and alkene ozonolysis as the major radical sources; NO_x termination and reservoir species were mainly nitric acid (HNO_3) and peroxy acetyl nitrate (PAN).[43] During the 2013 DISCOVER-AQ campaign, a young agricultural plume sampled in the southeast U.S. was analyzed using a box model and detailed VOC observations.[44] Elevated PAN mixing ratios downwind of two fires in the western U.S. and 15 agricultural fires in the southeastern U.S. were observed during the 2013 SEAC[4] RS campaign, indicating a significant NO_x sink.[17,45] Most recently during the 2018 WE-CAN campaign in the northwestern U.S., HONO observations in wildfire BB plumes indicated HONO photolysis as a dominant primary HO_x (=OH + HO_2) source in early plume evolution.[23,46]

We present an analysis of aircraft measurements that includes detailed chemistry to constrain O_3 production and its sensitivities in BB plumes. In the summer of 2019, a major field campaign sampled tens of wildfires in the western U.S. The Fire Influence on Regional to global Environments and Air Quality (FIREX-AQ) deployed the NASA DC-8 and the NOAA Twin Otter research aircraft to sample wildfire plumes. We use the initial emissions and downwind chemical transformation as sampled by the NOAA Twin Otter to investigate O_3 formation. We show a detailed investigation of the NO_x−VOC sensitivity of O_3 production during the first 2 h of plume evolution together with the primary HO_x sources and radical sinks in the sampled plumes.

2. METHODS

2.1. Platform and Instrumentation. Measurements were conducted in situ from the NOAA Twin Otter during FIREX-AQ from 29 July to 5 September 2019. The aircraft was based in Boise, ID, from 29 July to 5 September, and briefly in Cedar City, UT, from 19 August to 23 August. We focus on relevant measurements of wildfire plumes including their chemical, physical, and optical characterizations. A summary of the measurements including methods, sampling frequency, uncertainties, and references used for this analysis is presented in Table 1. More information and data can be found at https://csl.noaa.gov/projects/firex-aq/twinotterCHEM/.

2.2. Selected Fires and Plume Intercepts. The NOAA Twin Otter sampled western wildfires during 40 research flights. We present the analysis of 11 research flights sampling seven fire complexes, which were selected for the time of day, the number of downwind transects, and full data coverage (map shown in Figure 1a). The dates, names, time of day, fuels, locations, burn size, GOES-16 24 h mean fire radiative power (FRP), average photolysis rate, number of plume transects, and histograms of CO are included in the Supporting Information (Table S1 and Figure S22).

The NOAA Twin Otter probed air masses as they advected downwind to investigate the chemical evolution with time. However, it not possible to maintain Lagrangian sampling (i.e., repeat sampling of the same air mass) in complex plume structure, terrain, and airspace. Thus, we deem our approach "semi-Lagrangian". The average true airspeed for plume transects was 71 ± 0.2 m s^{-1}, yielding a spatial resolution of ∼70 m for 1 Hz instruments. A typical time series obtained during a semi-Lagrangian experiment is included in the Supporting Information (Figure S1).

2.3. Plume Ages. Plume ages were calculated taking both advection and plume rise into account.[58] Advection was determined using back trajectories from HYSPLIT using three different meteorological fields (HRRR 3 km, NAM CONUS nest 3 km, and GFS 0.25°). Vertical plume rise time was based on the height of the trajectory above the surface at the point in which it most closely approached the fire complex with an assumed mean vertical rise speed of 7 m s^{-1} (50 ± 5% of total transport speed). Uncertainty in plume age is estimated from the range in ages computed with the three meteorological fields, with median uncertainty around 25% of the age. The age at the center of the plume (highest CO mixing ratio) was used for subsequent box modeling.

2.4. Photochemical Box Modeling. We simulated O_3 formation in BB plumes using the Framework for 0-D Atmospheric Modeling,[59] a photochemical zero-dimensional (0-D) box model. Near-field plume transects were limited by flight restrictions; thus, an iterative box model[60,61] was applied to investigate early plume chemistry. The gas-phase chemical mechanism implemented in this 0-D model was adapted from the Master Chemical Mechanism (MCMv3.3.1) with additional BBVOC oxidation reactions for furan, 2-methylfuran, 3-methylfuran, 2,5-dimethylfuran, furfural, 5-methylfurfural, methylguaiacol, guaiacol, and syringol.[23,62] Catechol, methyl catechol, dimethyl catechol, and benzoquinone oxidation were also updated in the MCM as described in the Supporting Information (Figure S2) based on experimental work by Finewax et al.[63] and Schwantes et al.[64] The MCM with additional BBVOCs[23,62] is a near-explicit mechanism used to characterize the gas-phase chemical processes involved in the degradation of over 143 VOCs.[65,66]

BBVOC emissions have been studied extensively as a function of both combustion conditions and fuel types commonly found in the western U.S.[21−23,25,32,62,67] In this work, a VOC emissions profile was developed using data compiled by Decker et al.,[62] based on measurements made during the 2012 FLAME-IV[21] and 2016 FIREX[22] (hereafter referred to as FIRELAB) laboratory experiments. This dataset comprises 302 of the most reactive BBVOCs measured at FIRELAB, and we use 48 of the most abundant in this study. The variability of VOC emissions was investigated by comparing the FIRELAB emissions ratio data[32] to the FIREX-AQ 2019 DC-8 observations and the 2012 FLAME-IV lab experiment to find an agreement within a factor of 2 among all studies (see Figures S3 and S4). Following these comparisons, the FIRELAB BBVOC emission profile was extended to an additional VOC emissions profile in which the FIRELAB BBVOC emissions were reduced by 50% as an extra VOC sensitivity case study (referred to as 0.5 FIRELAB) (Table S3).

The model was initialized using measured mixing ratios of NO, NO_2, HONO, O_3, CO, CH_4, C_6H_6O (phenol), $C_6H_6O_2$ (catechol), and C_7H_8O (cresol) (see Table 1) measured at the densest part of the plume, as determined by the highest CO mixing ratio. This approach does not account for the plume center to edge variability in photochemical regimes. The low time resolution of the BBVOC data measured by two-dimensional (2-D) gas chromatography−mass spectrometry (GC−MS) required the use of derived VOC emissions profiles to initialize the model. Time-dependent BBVOC mixing ratios, based on the profiles described above, were compared with

https://doi.org/10.1021/acs.est.1c01963
Environ. Sci. Technol. XXXX, XXX, XXX−XXX

observed BBVOCs from the I^- CIMS and 2-D GC−MS. The measured BBVOCs are in better agreement with the reduced VOC emissions profile (0.5 FIRELAB) (Figures S5, S6, and S13−S21) and the results from this profile are reported herein. The better agreement with the 0.5 FIRELAB case is possibly due to differences in modified combustion efficiency (MCE) between laboratory studies (0.93 ± 0.02)[68] and real fire emissions (this study: 0.89 ± 0.02; see Table S1); however, MCE relationships with VOC emissions are generally complex and sometimes poorly correlated.[68−70]

Dilution is an important physical process influencing the chemical evolution of fire plumes. An approximately conserved tracer (CO) was used to determine a first-order loss rate (k_{dil}), which is applied to all chemical species in the box model. In some instances, regional background air had higher mixing ratios than in the plume for certain species (CO_2, O_3), in which case, dilution caused a mass increase of species into the plume.[71] Background mixing ratios were constrained to measurements made immediately outside of the plume for each flight (see Table S2 for k_{dil} and average background mixing ratios).

We developed a numerical iteration scheme to estimate the initial conditions required to fit observations downwind of each fire (description and model fit examples in Supporting Information Figures S5 and S6). Emission scaling factors for CO, NO_x, HONO, and the entire VOC profile are reported in the Supporting Information (Table S3). Additionally, HONO-to-NO_x ratios (ppbv/ppbv) are provided after 30 min of oxidation (Table S3). The modeled fire plumes had an average HONO-to-NO_x ratio of 0.12 ± 0.21 after 30 min of oxidation, which is within the range of reported laboratory and field-based studies.[19,20,46] Generally, the modeled plumes underestimated first transect HONO-to-NO_x ratio observations made on the NOAA Twin Otter (0.21 ± 0.11).

In addition to chemical constraints, the model was constrained with measured meteorological parameters (temperature, pressure, relative humidity, solar zenith angle, and NO_2 photolysis rate). Photolysis rates were constrained with the MCM parameterization[65] and then scaled to the observed jNO_2 measurements. This scaling approach allows the model to account for the plume darkening effect on photolysis rates, but does not account for spectral dependence. Stronger attenuation at shorter wavelengths may reduce photolysis rates for UV-absorbing molecules such as O_3, HCHO, or HONO smaller than modeled.

3. RESULTS AND DISCUSSION

The western wildfire plumes sampled from the Twin Otter in summer 2019 exhibited rapid photochemical production of O_3. Most of these plumes were from moderately sized fires (GOES-16 FRP 24 h mean range: 61−643 MW) that were not optically opaque, with average relative reductions in NO_2 photolysis rates of 27 ± 22% at the plume center, where the range represents one standard deviation of the mean. Results for more optically dense plumes from larger fires are likely to be different. Generally, both sets of models represented O_3 mixing ratios downwind (average error ± standard deviation); the 0.5 FIRELAB (overall: 0.6 ± 4%) profile matched initial plume transects (3.7 ± 7%) more accurately than the FIRELAB (1st transect: 14 ± 16%) profile (overall: 5.1 ± 7%) (see Table S5). Modeled maximum O_3 mixing ratios were reached within 60 min of emission for all modeled plumes. Initial O_3 production rates (initial maximum slopes of Figure 2a) of afternoon plumes (12:00−17:00 MDT) were, on average, higher than evening plumes (17:00−20:45 MDT)

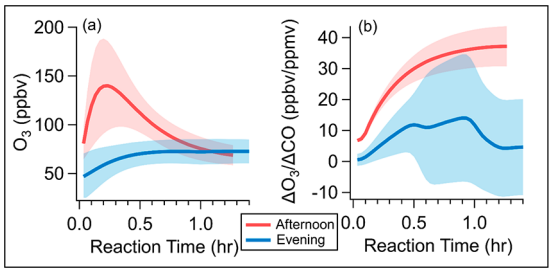

Figure 2. Modeled O_3 mixing ratio using the 0.5 FIRELAB BBVOC emissions case. (a) Modeled O_3 mixing ratio as a function of reaction time for all modeled fires averaged by time of day sampled. Shading represents one standard deviation. (b) Modeled normalized excess O_3 mixing ratio as a function of reaction time for all modeled fires averaged by time of day sampled. Shading represents one standard deviation. Modeled O_x (O_3 + NO_2) and normalized excess O_x mixing ratios as a function of reaction time display similar trends as NO_2 makes up ∼10% of O_x (Figures S11 and S12).

(500 ± 60 and 66 ± 2 ppbv h^{-1}, respectively). These daytime O_3 production rates are large compared to urban O_3 production, which is typically 10−100 ppbv h^{-1} near source regions.[72−75] Modeled afternoon plumes reached an average maximum O_3 mixing ratio of 140 ± 50 ppbv within 20 ± 10 min of emission compared to 76 ± 12 ppbv in 60 ± 30 min in evening plumes. The model exhibited more pronounced, rapid photochemical production of O_3 in afternoon plumes due to rapid production of primary radicals that initiate oxidation reactions in the NO_x−HO_x cycle. On average, afternoon fire plumes produced twice as much O_3 in half the time as evening plumes. Dilution rates in the observed BB plumes were competitive with O_3 production rates, oftentimes making O_3 enhancements within the plume relatively small several hours downwind. The normalized excess mixing ratio (NEMR) accounts for plume dilution and entrainment of background air into the plume.

$$\mathrm{NEMR}_{O_3} = \frac{\Delta O_3}{\Delta CO} = \frac{(O_{3\,\mathrm{plume}} - O_{3\,\mathrm{background}})}{(CO_{\mathrm{plume}} - CO_{\mathrm{background}})}$$

The highest $NEMR_{O_3}$ rate (maximum slope in Figure 2b) was observed in the afternoon plumes, reaching 65 ± 3 ppbv O_3 ppmv CO^{-1} h^{-1} (Figure 2b). The evening $NEMR_{O_3}$ rate reached a maximum on average of 43 ± 1 ppmv O_3 ppbv CO^{-1} h^{-1} (Figure 2b).

The NO_x−VOC sensitivity of O_3 production for an individual plume determines both O_3 production rates and response to the emissions from specific fires. A common tool used for understanding the nonlinear relationship between O_3, NO_x, and VOC is the O_3 isopleth. This analysis method has seen numerous applications to O_3 sensitivities in urban areas,[26,76] oil- and gas-producing regions,[28,77] and NO_x-impacted, biogenic-rich environments,[78] but is less common in the analysis of fire plumes.[39] Fires differ from anthropogenic sources in two respects. First, BBVOC emissions differ markedly from urban or biogenic VOCs, with BBVOC reactivity dominated by species such as oxygenated and nonoxygenated aromatics, furans, and terpenes.[22] Second, $BBNO_x$ emissions vary and depend on both fuel nitrogen

https://doi.org/10.1021/acs.est.1c01963
Environ. Sci. Technol. XXXX, XXX, XXX−XXX

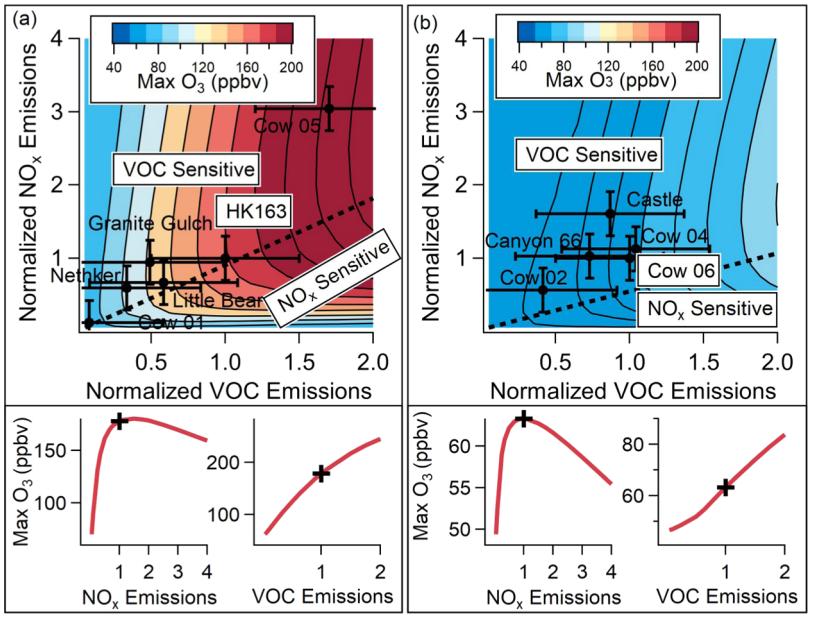

Figure 3. Isopleths of maximum modeled O_3 for two BB wildfire plumes utilizing a 0.5 FIRELAB VOC profile. Black dashed lines indicate maxima in NO_x sensitivity. (a) Modeled HK163 afternoon plume maximum O_3 isopleth as a function of normalized NO_x and VOC base emissions. Each marker represents individual afternoon plumes in relative NO_x–VOC space, with error bars representing measurement error for NO_x (including HONO) and 50% error for VOCs (to encompass both VOC profiles). Below the isopleth shows cuts through the afternoon isopleth at the HK163 base case with normalized NO_x and VOC emissions of 1. (b) Modeled Cow 06 evening plume maximum O_3 isopleth, as a function of normalized NO_x and VOC base emissions. Each marker represents evening plumes in relative NO_x–VOC space. Below the isopleth shows cuts through the evening isopleth at the Cow 06 base case with normalized NO_x and VOC emissions of 1.

content and fire stage (e.g., flaming or smoldering),[20] leading to potentially large variability in plume O_3 production.

The HK163 and Cow 06 fires were chosen as base cases to represent the median NO_x and VOC emissions for afternoon and evening populations. Emissions in the model (NO_x + HONO and VOCs) are varied to determine the effect on O_3 production in these BB plumes (for maximum O_3 isopleths, see Figure 3). The relative VOC profile (including HCHO) for every model run was kept constant, which made it possible to plot all of the afternoon and evening fires on each isopleth, respectively. Both afternoon and evening fires fell in the VOC-sensitive regime of the maximum O_3 isopleth, but were close to the NO_x-sensitive transition line (Figure 3). This result is surprising because fire emissions are expected to have high VOC and low NO_x emissions.[17] The modeled average initial VOC-to-NO_x ratio (including HONO) was 30 ± 40 and 44 ± 20 ppbv C ppbv NO_x^{-1} for afternoon and evening plumes, respectively. In contrast, urban plumes as reported by Mao et al.[34] have generally lower average VOC-to-NO_x ratios (24 ± 10 ppbv C ppbv NO_x^{-1}).

3.1. Modeled Radical Budget. Maximum O_3 isopleths describe only one point in a plume's chemical evolution. It is useful to investigate NO_x–VOC sensitivities as the plume advects downwind. The NO_x–VOC sensitivities of photochemical O_3 production can also be expressed in terms of the sources and sinks of free radicals (HO_x + RO + RO_2). The largest radical source in the lower atmosphere is the photolysis of O_3 at wavelengths shorter than 340 nm, which yields excited oxygen atoms, $O^1(D)$, that react with water vapor to produce hydroxyl radicals.[79] Biomass burning, by contrast, directly emits photolytic radical precursors, such as HONO and HCHO. Photolysis of HONO, HCHO, other aldehydes, and acetone, along with the ozonolysis of alkenes,[42,46,80] leads to rapid HO_x production early in the evolution of fire plumes. Large radical sources, in turn, tend to force O_3 production into the NO_x sensitive regime.[30,34] While many of the same radical sources also influence urban air, they are not emitted at the concentrated levels found in early fire plume evolution. Peak actinic flux and FRP (proxy for emissions) both occur during the afternoon hours (Figure 1b), allowing for rapid HO_x production. During the evening hours, actinic flux decreases much more rapidly than FRP, reducing HO_x production and O_3 production during potentially sustained emissions.

The afternoon plumes' primary HO_x (pHO_x) budget was dominated by HONO photolysis, making up 48 ± 20% (average ± standard deviation) (Figure 4a). The second most important production term to the afternoon pHO_x budget was HCHO photolysis (26 ± 9%); HCHO emissions were purely based on emissions databases; thus, the uncertainty with this radical source is high. The remainder of the pHO_x budget for afternoon plumes was made up of aldehyde photolysis, alkene ozonolysis, and $O(^1D)$ (10 ± 3, 7 ± 5, and 5 ± 5% respectively). The top three contributors to evening plumes' pHO_x budget were HONO photolysis (53 ± 7%), HCHO photolysis (18 ± 9%), and alkene ozonolysis (17 ± 9%). The pHO_x budget for the FIRELAB emissions case differs markedly (Figure S7), with HO_x production in afternoon plumes led by HCHO photolysis (46 ± 3%), alkene ozonolysis (16 ± 3%), and HONO photolysis (13 ± 4%).

In addition to these rapid primary HO_x sources, the rate at which radicals are terminated by NO_x is another critical aspect of O_3 production efficiency.[30] Net O_3 production from NO_x cycling between NO and NO_2 is related to the coupled chain length of the HO_x cycle interconverting OH, HO_2, and RO_2. This chain propagation is characterized by the OH or HO_x chain length, with longer chain lengths resulting in more oxidative cycles per OH or HO_2 radical, producing more O_3.[34,81] There are two channels of termination reactions, self-

https://doi.org/10.1021/acs.est.1c01963
Environ. Sci. Technol. XXXX, XXX, XXX−XXX

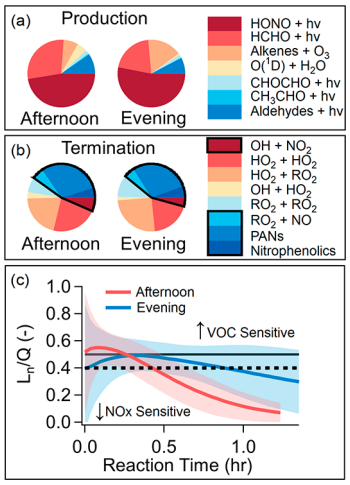

Figure 4. Primary HO_x (OH + HO_2) production and radical termination budgets for the 0.5 FIRELAB VOC profile. (a) Average integrated afternoon and evening plume primary HO_x production. (b) Average integrated afternoon and evening plume radical termination budgets, with L_n terms outlined in black. (c) Average afternoon and evening L_n/Q time series with one standard deviation shading and NO_x sensitivity transition shown with black dashed trace (L_n/Q = 0.41) and black solid trace (L_n/Q = 0.5).

termination, where radicals react with themselves, and reactions of radicals with NO_x, which remove both species from the propagation cycle. The formation of nitrophenolics is a chain termination reaction that is prevalent in BB plumes[63] but is minor in polluted urban areas.[82] Phenolic compounds are large BBVOC emissions whose oxidation to phenoxy radicals removes NO_2 from the system without producing O_3.[23]

Integrated radical termination (Figure 4b) was split equally between radical loss to NO_x and radical−radical reactions in both afternoon and evening plumes. In afternoon plumes, the radical loss to NO_x was almost half (47 ± 7%) of the termination budget compared to 43 ± 6% for evening plumes, and in both afternoon and evening plumes, it was led by PAN formation (30 ± 6 and 28 ± 3%, respectively). Plumes were sampled in an altitude range of 2200−4100 m and varied in temperature from 275 to 292 K, yielding thermal PAN lifetimes of 1.7−26 h, respectively. NO_x termination products in these plumes are HNO_3 (7 ± 1 and 4 ± 2% of the termination products for afternoon and evening, respectively), organic nitrates (6 ± 1 and 5 ± 1%), and nitrophenolics (5 ± 2 and 6 ± 5%). Nitrophenolics are considered permanent here in that their photolysis does not regenerate NO_x, as has been suggested,[83] although nitrophenolic photochemistry requires further investigation. As the production of nitrophenolics was determined via the phenoxy radical + NO_2 pathway, this termination term includes both OH and NO_3 initiated H-atom abstraction.

The NOAA Twin Otter had limited observations of NO_x oxidation products, mostly missing PAN. We present the available comparisons of modeled gas-phase HNO_3 to inorganic particulate nitrate (pNO_3), modeled and measured gas-phase organic nitrates (C5 isoprene hydroxy nitrates), and modeled 4-nitrocatechol (4-NC) expected to be in the particulate phase ($C^* \sim 14\ \mu g\ m^{-3}$, 78 ± 10% of 4-NC should be particle bound)[63] to a particulate nitrocatechol ion marker, $pC_6H_5NO_4^+$, for a single flight in the Supporting Information (Figure S8). The comparisons of HNO_3 with pNO_3 and between the C5 gas-phase nitrates are quite favorable, and both 4-NC and $pC_6H_5NO_4^+$ show similar trends with reaction time. However, the 4-NC comparison is not quantitative here because a calibration of particulate 4-NC with our AMS instrument is not available. Further work on the 4-NC comparison may highlight the uncertainty in the current understanding of nitrophenolic photolysis, as well as gas-phase and heterogeneous-uptake chemistry.[83,84]

The relative rates of radical production and termination provide a measure of the NO_x sensitivity of O_3 formation that is independent of an isopleth calculation and can be evaluated instantaneously along a modeled plume's O_3 trajectory. The balance between radical production and termination at any point in the plume can be described by the parameter L_n/Q.[27,30,85]

$$L_n = P(HNO_3) + P(RONO_2) + P(PAN) + P(\text{nitrophenolics})$$

$$Q = L_r + L_n$$

The term L_n is the rate of radical (OH, RO, RO_2) removal by reactions with NO_x, L_r is the rate of self-radical removal (OH + HO_2, RO_2 + RO_2, etc.) and Q is the sum of all radical loss.[27] Classically, a plume is considered VOC-sensitive when the majority of radical termination proceeds via reactions with NO_x or when $L_n/Q > 0.5$.[27] Additionally, a plume is NO_x-sensitive when $L_n/Q < 0.5$ or when radical−radical reactions govern radical chain termination.[27] However, when additional L_n terms are added to the analysis (such as PAN or nitrophenolics), the transition from VOC- to NO_x-sensitive chemistry can differ from the classical definition.[86] An analysis of both afternoon and evening isopleths yield an L_n/Q transition of 0.41 for BB chemistry (Figures S9 and S10). As evidenced by their L_n/Q time series, afternoon plumes transitioned from near-maximum NO_x efficiency to NO_x-sensitive chemistry downwind, on average after 26 min of photochemistry (Figure 4c). Not only was the transition rapid, but after 1.25 h of photochemistry, modeled L_n/Q values for afternoon plumes reached 0.07 ± 0.1, or strongly NO_x-sensitive. Meanwhile, evening plumes remained close to maximum NO_x efficiency for the duration of this analysis (Figure 4c) with a maximum in L_n/Q after 22 min of photochemistry. Thus, evening plumes demonstrated a slower transition to NO_x-sensitive O_3 production than afternoon plumes. The evening transition to NO_x-sensitive O_3 production was less drastic than in the afternoon plumes, with average L_n/Q values at 1.25 h of 0.29 ± 0.2.

This study emphasizes the importance of time-of-day parameterization of BB plume O_3 production in chemical models. Afternoon plumes demonstrated a rapid transition to NO_x-sensitive O_3 production and sequestered NO_x in the form of PANs, organic nitrates, HNO_3, and nitrophenolic compounds. Interestingly, PAN formation is quite similar for both VOC profiles. The similarity may be due to substantial secondary acetaldehyde production (compensating for differences in initial VOC emissions) or differences in initial NO_2 emissions for each VOC profile. As a fire emits into the evening hours, reduction of photolysis rates and emissions of radical precursors limit the production of primary radicals, slowing the transition to NO_x-sensitive chemistry. Fire plumes much larger than those sampled by the NOAA Twin Otter may exhibit aspects of evening plume chemistry due to large

https://doi.org/10.1021/acs.est.1c01963
Environ. Sci. Technol. XXXX, XXX, XXX−XXX

reductions in photolysis rates. Further validations of the NOAA BB chemical mechanism for NO_x oxidation products (i.e., organic nitrates, nitrophenolics) and loss mechanisms will be important to improving chemical models of BB plumes. Due to the near-field (<2 h) focus of this analysis, an important extension of this work is to understand how BB plumes interact with urban NO_x and radical sources many hours downwind. The NO_x sensitivity in even moderately aged plumes suggests the potential for efficient O_3 production through interactions with urban emissions.

■ ASSOCIATED CONTENT

Supporting Information

The Supporting Information is available free of charge at https://pubs.acs.org/doi/10.1021/acs.est.1c01963.

Extended experimental methods, expansion of phenolic mechanism description, and additional VOC profile results as well as Tables S1−S4 and Figures S1−S8 (PDF)

■ AUTHOR INFORMATION

Corresponding Author

Steven S. Brown − *NOAA Chemical Sciences Laboratory, Boulder, Colorado 80305, United States; Department of Chemistry, University of Colorado Boulder, Boulder, Colorado 80309, United States;* orcid.org/0000-0001-7477-9078; Email: steven.s.brown@noaa.gov

Authors

Michael A. Robinson − *NOAA Chemical Sciences Laboratory, Boulder, Colorado 80305, United States; Cooperative Institute for Research in Environmental Sciences, University of Colorado Boulder, Boulder, Colorado 80309, United States; Department of Chemistry, University of Colorado Boulder, Boulder, Colorado 80309, United States;* orcid.org/0000-0003-0977-9148

Zachary C. J. Decker − *NOAA Chemical Sciences Laboratory, Boulder, Colorado 80305, United States; Cooperative Institute for Research in Environmental Sciences, University of Colorado Boulder, Boulder, Colorado 80309, United States; Department of Chemistry, University of Colorado Boulder, Boulder, Colorado 80309, United States;* orcid.org/0000-0001-9604-8671

Kelley C. Barsanti − *Department of Chemical and Environmental Engineering and College of Engineering-Center for Environmental Research and Technology (CE-CERT), University of California, Riverside, Riverside, California 92507, United States;* orcid.org/0000-0002-6065-8643

Matthew M. Coggon − *NOAA Chemical Sciences Laboratory, Boulder, Colorado 80305, United States; Cooperative Institute for Research in Environmental Sciences, University of Colorado Boulder, Boulder, Colorado 80309, United States;* orcid.org/0000-0002-5763-1925

Frank M. Flocke − *Atmospheric Chemistry Observations and Modeling Laboratory, National Center for Atmospheric Research, Boulder, Colorado 80301, United States*

Alessandro Franchin − *NOAA Chemical Sciences Laboratory, Boulder, Colorado 80305, United States; Cooperative Institute for Research in Environmental Sciences, University of Colorado Boulder, Boulder, Colorado 80309, United States;* Present Address: Atmospheric Chemistry Observations and Modeling Laboratory, National Center for Atmospheric Research, Boulder, Colorado 80301, United States

Carley D. Fredrickson − *Department of Atmospheric Sciences, University of Washington, Seattle, Washington 98195, United States*

Jessica B. Gilman − *NOAA Chemical Sciences Laboratory, Boulder, Colorado 80305, United States*

Georgios I. Gkatzelis − *NOAA Chemical Sciences Laboratory, Boulder, Colorado 80305, United States; Cooperative Institute for Research in Environmental Sciences, University of Colorado Boulder, Boulder, Colorado 80309, United States;* Present Address: Institute of Energy and Climate Research, IEK-8: Troposphere, Forschungszentrum Jülich GmbH, 52425 Jülich, Germany.

Christopher D. Holmes − *Department of Earth, Ocean and Atmospheric Science, Florida State University, Tallahassee, Florida 32306, United States;* orcid.org/0000-0002-2727-0954

Aaron Lamplugh − *NOAA Chemical Sciences Laboratory, Boulder, Colorado 80305, United States; Cooperative Institute for Research in Environmental Sciences, University of Colorado Boulder, Boulder, Colorado 80309, United States*

Avi Lavi − *Department of Chemical and Environmental Engineering and College of Engineering-Center for Environmental Research and Technology (CE-CERT), University of California, Riverside, Riverside, California 92507, United States;* Present Address: South Coast Air Quality Management, Diamond Bar, California 91765, United States.

Ann M. Middlebrook − *NOAA Chemical Sciences Laboratory, Boulder, Colorado 80305, United States*

Denise M. Montzka − *Atmospheric Chemistry Observations and Modeling Laboratory, National Center for Atmospheric Research, Boulder, Colorado 80301, United States*

Brett B. Palm − *Department of Atmospheric Sciences, University of Washington, Seattle, Washington 98195, United States*

Jeff Peischl − *NOAA Chemical Sciences Laboratory, Boulder, Colorado 80305, United States; Cooperative Institute for Research in Environmental Sciences, University of Colorado Boulder, Boulder, Colorado 80309, United States*

Brad Pierce − *Space Science and Engineering Center, University of Wisconsin−Madison, Madison, Wisconsin 53715, United States*

Rebecca H. Schwantes − *NOAA Chemical Sciences Laboratory, Boulder, Colorado 80305, United States; Cooperative Institute for Research in Environmental Sciences, University of Colorado Boulder, Boulder, Colorado 80309, United States*

Kanako Sekimoto − *Graduate School of Nanobioscience, Yokohama City University, Yokohama, Kanagawa 236-0027, Japan;* orcid.org/0000-0001-9908-9698

Vanessa Selimovic − *Department of Chemistry and Biochemistry, University of Montana, Missoula, Montana 59812, United States*

Geoffrey S. Tyndall − *Atmospheric Chemistry Observations and Modeling Laboratory, National Center for Atmospheric Research, Boulder, Colorado 80301, United States*

Joel A. Thornton − *Department of Atmospheric Sciences, University of Washington, Seattle, Washington 98195, United States*

Paul Van Rooy − *Department of Chemical and Environmental Engineering and College of Engineering-Center for*

https://doi.org/10.1021/acs.est.1c01963
Environ. Sci. Technol. XXXX, XXX, XXX−XXX

Environmental Research and Technology (CE-CERT), University of California, Riverside, Riverside, California 92507, United States

Carsten Warneke − *NOAA Chemical Sciences Laboratory, Boulder, Colorado 80305, United States;* orcid.org/0000-0003-3811-8496

Andrew J. Weinheimer − *Atmospheric Chemistry Observations and Modeling Laboratory, National Center for Atmospheric Research, Boulder, Colorado 80301, United States*

Complete contact information is available at: https://pubs.acs.org/10.1021/acs.est.1c01963

Notes

The authors declare no competing financial interest.

■ ACKNOWLEDGMENTS

The authors thank all those who helped organize and participated in the 2019 FIREX-AQ field campaign. They also thank Amber Soja and Emily Gargulinski for compiling ecosystem and fire burned area data. They thank NOAA Aircraft Operations, particularly, Francisco Fuenmayor, Joe Greene, Conor Maginn, Rob Miletic, Joshua Rannenberg, and David Reymore. J.A.T., C.D.F., and B.B.P. were supported by a grant from the National Oceanic and Atmospheric Administration (NA17OAR4310012). C.D.H. was supported by a grant from the National Aeronautics and Space Administration (80NSSC18K0625). The authors acknowledge Andrew Rollins and Caroline Womack for helpful discussions.

■ REFERENCES

(1) Lindaas, J.; Farmer, D. K.; Pollack, I. B.; Abeleira, A.; Flocke, F.; Roscioli, R.; Herndon, S.; Fischer, E. V. Changes in Ozone and Precursors during Two Aged Wildfire Smoke Events in the Colorado Front Range in Summer 2015. *Atmos. Chem. Phys.* **2017**, *17*, 10691−10707.

(2) Baylon, P.; Jaffe, D. A.; Wigder, N. L.; Gao, H.; Hee, J. Ozone Enhancement in Western US Wildfire Plumes at the Mt. Bachelor Observatory: The Role of NOx. *Atmos. Environ.* **2015**, *109*, 297−304.

(3) Jaffe, D.; Chand, D.; Hafner, W.; Westerling, A.; Spracklen, D. Influence of Fires on O_3 Concentrations in the Western U.S. *Environ. Sci. Technol.* **2008**, *42*, 5885−5891.

(4) Cooper, O. R.; Gao, R.-S.; Tarasick, D.; Leblanc, T.; Sweeney, C. Long-Term Ozone Trends at Rural Ozone Monitoring Sites across the United States, 1990-2010: RURAL U.S. OZONE TRENDS, 1990-2010. *J. Geophys. Res.* **2012**, *117*, No. D22307.

(5) Cooper, O. R.; Langford, A. O.; Parrish, D. D.; Fahey, D. W. Challenges of a Lowered U.S. Ozone Standard. *Science* **2015**, *348*, 1096−1097.

(6) Brey, S. J.; Fischer, E. V. Smoke in the City: How Often and Where Does Smoke Impact Summertime Ozone in the United States? *Environ. Sci. Technol.* **2016**, *50*, 1288−1294.

(7) Lu, X.; Zhang, L.; Yue, X.; Zhang, J.; Jaffe, D. A.; Stohl, A.; Zhao, Y.; Shao, J. Wildfire Influences on the Variability and Trend of Summer Surface Ozone in the Mountainous Western United States. *Atmos. Chem. Phys.* **2016**, *16*, 14687−14702.

(8) Chameides, W. L. The Photochemical Role of Tropospheric Nitrogen Oxides. *Geophys. Res. Lett.* **1978**, *5*, 17−20.

(9) Crutzen, P. J. The Influence of Nitrogen Oxides on the Atmospheric Ozone Content. *Q. J. R. Meteorol. Soc.* **1970**, *96*, 320−325.

(10) Langmann, B.; Duncan, B.; Textor, C.; Trentmann, J.; van der Werf, G. R. Vegetation Fire Emissions and Their Impact on Air Pollution and Climate. *Atmos. Environ.* **2009**, *43*, 107−116.

(11) US EPA. 2017 National Emissions Inventory (NEI) Data. https://www.epa.gov/air-emissions-inventories/2017-national-emissions-inventory-nei-data (accessed December 28, 2020).

(12) Gillett, N. P. Detecting the Effect of Climate Change on Canadian Forest Fires. *Geophys. Res. Lett.* **2004**, *31*, No. L18211.

(13) Westerling, A. L. Warming and Earlier Spring Increase Western U.S. Forest Wildfire Activity. *Science* **2006**, *313*, 940−943.

(14) Westerling, A. L. Increasing Western US Forest Wildfire Activity: Sensitivity to Changes in the Timing of Spring. *Philos. Trans. R. Soc. B* **2016**, *371*, No. 20150178.

(15) Balch, J. K.; Bradley, B. A.; Abatzoglou, J. T.; Nagy, R. C.; Fusco, E. J.; Mahood, A. L. Human-Started Wildfires Expand the Fire Niche across the United States. *Proc. Natl. Acad. Sci. U.S.A.* **2017**, *114*, 2946−2951.

(16) Abatzoglou, J. T.; Williams, A. P. Impact of Anthropogenic Climate Change on Wildfire across Western US Forests. *Proc. Natl. Acad. Sci. U.S.A.* **2016**, *113*, 11770−11775.

(17) Liu, X.; Huey, L. G.; Yokelson, R. J.; Selimovic, V.; Simpson, I. J.; Müller, M.; Jimenez, J. L.; Campuzano-Jost, P.; Beyersdorf, A. J.; Blake, D. R.; Butterfield, Z.; Choi, Y.; Crounse, J. D.; Day, D. A.; Diskin, G. S.; Dubey, M. K.; Fortner, E.; Hanisco, T. F.; Hu, W.; King, L. E.; Kleinman, L.; Meinardi, S.; Mikoviny, T.; Onasch, T. B.; Palm, B. B.; Peischl, J.; Pollack, I. B.; Ryerson, T. B.; Sachse, G. W.; Sedlacek, A. J.; Shilling, J. E.; Springston, S.; St Clair, J. M.; Tanner, D. J.; Teng, A. P.; Wennberg, P. O.; Wisthaler, A.; Wolfe, G. M. Airborne Measurements of Western U.S. Wildfire Emissions: Comparison with Prescribed Burning and Air Quality Implications. *J. Geophys. Res.* **2017**, *122*, 6108−6129.

(18) Andreae, M. O. Emission of Trace Gases and Aerosols from Biomass Burning − an Updated Assessment. *Atmos. Chem. Phys.* **2019**, *19*, 8523−8546.

(19) Akagi, S. K.; Yokelson, R. J.; Burling, I. R.; Meinardi, S.; Simpson, I.; Blake, D. R.; McMeeking, G. R.; Sullivan, A.; Lee, T.; Kreidenweis, S.; Urbanski, S.; Reardon, J.; Griffith, D. W. T.; Johnson, T. J.; Weise, D. R. Measurements of Reactive Trace Gases and Variable O_3 Formation Rates in Some South Carolina Biomass Burning Plumes. *Atmos. Chem. Phys.* **2013**, *13*, 1141−1165.

(20) Roberts, J. M.; Stockwell, C. E.; Yokelson, R. J.; de Gouw, J.; Liu, Y.; Selimovic, V.; Koss, A. R.; Sekimoto, K.; Coggon, M. M.; Yuan, B.; Zarzana, K. J.; Brown, S. S.; Santin, C.; Doerr, S. H.; Warneke, C. The Nitrogen Budget of Laboratory-Simulated Western US Wildfires during the FIREX 2016 Fire Lab Study. *Atmos. Chem. Phys.* **2020**, *20*, 8807−8826.

(21) Hatch, L. E.; Yokelson, R. J.; Stockwell, C. E.; Veres, P. R.; Simpson, I. J.; Blake, D. R.; Orlando, J. J.; Barsanti, K. C. Multi-Instrument Comparison and Compilation of Non-Methane Organic Gas Emissions from Biomass Burning and Implications for Smoke-Derived Secondary Organic Aerosol Precursors. *Atmos. Chem. Phys.* **2017**, *17*, 1471−1489.

(22) Koss, A. R.; Sekimoto, K.; Gilman, J. B.; Selimovic, V.; Coggon, M. M.; Zarzana, K. J.; Yuan, B.; Lerner, B. M.; Brown, S. S.; Jimenez, J. L.; Krechmer, J.; Roberts, J. M.; Warneke, C.; Yokelson, R. J.; de Gouw, J. Non-Methane Organic Gas Emissions from Biomass Burning: Identification, Quantification, and Emission Factors from PTR-ToF during the FIREX 2016 Laboratory Experiment. *Atmos. Chem. Phys.* **2018**, *18*, 3299−3319.

(23) Coggon, M. M.; Lim, C. Y.; Koss, A. R.; Sekimoto, K.; Yuan, B.; Gilman, J. B.; Hagan, D. H.; Selimovic, V.; Zarzana, K. J.; Brown, S. S.; Roberts, J. M.; Müller, M.; Yokelson, R.; Wisthaler, A.; Krechmer, J. E.; Jimenez, J. L.; Cappa, C.; Kroll, J. H.; de Gouw, J.; Warneke, C. OH Chemistry of Non-Methane Organic Gases (NMOGs) Emitted from Laboratory and Ambient Biomass Burning Smoke: Evaluating the Influence of Furans and Oxygenated Aromatics on Ozone and Secondary NMOG Formation. *Atmos. Chem. Phys.* **2019**, *19*, 14875−14899.

(24) Stockwell, C. E.; Veres, P. R.; Williams, J.; Yokelson, R. J. Characterization of Biomass Burning Emissions from Cooking Fires, Peat, Crop Residue, and Other Fuels with High-Resolution Proton-

Transfer-Reaction Time-of-Flight Mass Spectrometry. *Atmos. Chem. Phys.* **2015**, *15*, 845−865.
(25) Gilman, J. B.; Lerner, B. M.; Kuster, W. C.; Goldan, P. D.; Warneke, C.; Veres, P. R.; Roberts, J. M.; de Gouw, J. A.; Burling, I. R.; Yokelson, R. J. Biomass Burning Emissions and Potential Air Quality Impacts of Volatile Organic Compounds and Other Trace Gases from Fuels Common in the US. *Atmos. Chem. Phys.* **2015**, *15*, 13915−13938.
(26) Seinfeld, J. H. Urban Air Pollution: State of the Science. *Science* **1989**, *243*, 745−752.
(27) Kleinman, L. I.; Daum, P. H.; Lee, J. H.; Lee, Y.-N.; Nunnermacker, L. J.; Springston, S. R.; Newman, L.; Weinstein-Lloyd, J.; Sillman, S. Dependence of Ozone Production on NO and Hydrocarbons in the Troposphere. *Geophys. Res. Lett.* **1997**, *24*, 2299−2302.
(28) Edwards, P. M.; Brown, S. S.; Roberts, J. M.; Ahmadov, R.; Banta, R. M.; deGouw, J. A.; Dubé, W. P.; Field, R. A.; Flynn, J. H.; Gilman, J. B.; Graus, M.; Helmig, D.; Koss, A.; Langford, A. O.; Lefer, B. L.; Lerner, B. M.; Li, R.; Li, S.-M.; McKeen, S. A.; Murphy, S. M.; Parrish, D. D.; Senff, C. J.; Soltis, J.; Stutz, J.; Sweeney, C.; Thompson, C. R.; Trainer, M. K.; Tsai, C.; Veres, P. R.; Washenfelder, R. A.; Warneke, C.; Wild, R. J.; Young, C. J.; Yuan, B.; Zamora, R. High Winter Ozone Pollution from Carbonyl Photolysis in an Oil and Gas Basin. *Nature* **2014**, *514*, 351−354.
(29) Mazzuca, G. M.; Ren, X.; Loughner, C. P.; Estes, M.; Crawford, J. H.; Pickering, K. E.; Weinheimer, A. J.; Dickerson, R. R. Ozone Production and Its Sensitivity to NO_X and VOCs: Results from the DISCOVER-AQ Field Experiment, Houston 2013. *Atmos. Chem. Phys.* **2016**, *16*, 14463−14474.
(30) Kleinman, L. I. The Dependence of Tropospheric Ozone Production Rate on Ozone Precursors. *Atmos. Environ.* **2005**, *39*, 575−586.
(31) Hornbrook, R. S.; Blake, D. R.; Diskin, G. S.; Fried, A.; Fuelberg, H. E.; Meinardi, S.; Mikoviny, T.; Richter, D.; Sachse, G. W.; Vay, S. A.; Walega, J.; Weibring, P.; Weinheimer, A. J.; Wiedinmyer, C.; Wisthaler, A.; Hills, A.; Riemer, D. D.; Apel, E. C. Observations of Nonmethane Organic Compounds during ARCTAS − Part 1: Biomass Burning Emissions and Plume Enhancements. *Atmos. Chem. Phys.* **2011**, *11*, 11103−11130.
(32) Hatch, L. E.; Jen, C. N.; Kreisberg, N. M.; Selimovic, V.; Yokelson, R. J.; Stamatis, C.; York, R. A.; Foster, D.; Stephens, S. L.; Goldstein, A. H.; Barsanti, K. C. Highly Speciated Measurements of Terpenoids Emitted from Laboratory and Mixed-Conifer Forest Prescribed Fires. *Environ. Sci. Technol.* **2019**, *53*, 9418−9428.
(33) Wood, E. C.; Herndon, S. C.; Onasch, T. B.; Kroll, J. H.; Canagaratna, M. R.; Kolb, C. E.; Worsnop, D. R.; Neuman, J. A.; Seila, R.; Zavala, M.; Knighton, W. B. A Case Study of Ozone Production, Nitrogen Oxides, and the Radical Budget in Mexico City. *Atmos. Chem. Phys.* **2009**, *9*, 2499−2516.
(34) Mao, J.; Ren, X.; Chen, S.; Brune, W. H.; Chen, Z.; Martinez, M.; Harder, H.; Lefer, B.; Rappenglück, B.; Flynn, J.; Leuchner, M. Atmospheric Oxidation Capacity in the Summer of Houston 2006: Comparison with Summer Measurements in Other Metropolitan Studies. *Atmos. Environ.* **2010**, *44*, 4107−4115.
(35) Volkamer, R.; Sheehy, P.; Molina, L. T.; Molina, M. J. Oxidative Capacity of the Mexico City Atmosphere − Part 1: A Radical Source Perspective. *Atmos. Chem. Phys.* **2010**, *10*, 6969−6991.
(36) Young, C. J.; Washenfelder, R. A.; Roberts, J. M.; Mielke, L. H.; Osthoff, H. D.; Tsai, C.; Pikelnaya, O.; Stutz, J.; Veres, P. R.; Cochran, A. K.; VandenBoer, T. C.; Flynn, J.; Grossberg, N.; Haman, C. L.; Lefer, B.; Stark, H.; Graus, M.; de Gouw, J.; Gilman, J. B.; Kuster, W. C.; Brown, S. S. Vertically Resolved Measurements of Nighttime Radical Reservoirs in Los Angeles and Their Contribution to the Urban Radical Budget. *Environ. Sci. Technol.* **2012**, *46*, 10965−10973.
(37) Lu, K.; Fuchs, H.; Hofzumahaus, A.; Tan, Z.; Wang, H.; Zhang, L.; Schmitt, S. H.; Rohrer, F.; Bohn, B.; Broch, S.; Dong, H.; Gkatzelis, G. I.; Hohaus, T.; Holland, F.; Li, X.; Liu, Y.; Liu, Y.; Ma, X.; Novelli, A.; Schlag, P.; Shao, M.; Wu, Y.; Wu, Z.; Zeng, L.; Hu, M.; Kiendler-Scharr, A.; Wahner, A.; Zhang, Y. Fast Photochemistry in Wintertime Haze: Consequences for Pollution Mitigation Strategies. *Environ. Sci. Technol.* **2019**, *53*, 10676−10684.
(38) Haskins, J. D.; Lopez-Hilfiker, F. D.; Lee, B. H.; Shah, V.; Wolfe, G. M.; DiGangi, J.; Fibiger, D.; McDuffie, E. E.; Veres, P.; Schroder, J. C.; Campuzano-Jost, P.; Day, D. A.; Jimenez, J. L.; Weinheimer, A.; Sparks, T.; Cohen, R. C.; Campos, T.; Sullivan, A.; Guo, H.; Weber, R.; Dibb, J.; Green, J.; Fiddler, M.; Bililign, S.; Jaeglé, L.; Brown, S. S.; Thornton, J. A. Anthropogenic Control Over Wintertime Oxidation of Atmospheric Pollutants. *Geophys. Res. Lett.* **2019**, *46*, 14826−14835.
(39) Poppe, D.; Koppmann, R.; Rudolph, J. Ozone Formation in Biomass Burning Plumes: Influence of Atmospheric Dilution. *Geophys. Res. Lett.* **1998**, *25*, 3823−3826.
(40) Mason, S. A.; Field, R. J.; Yokelson, R. J.; Kochivar, M. A.; Tinsley, M. R.; Ward, D. E.; Hao, W. M. Complex Effects Arising in Smoke Plume Simulations Due to Inclusion of Direct Emissions of Oxygenated Organic Species from Biomass Combustion. *J. Geophys. Res.* **2001**, *106*, 12527−12539.
(41) Jost, C.; Trentmann, J.; Sprung, D.; Andreae, M. O.; McQuaid, J. B.; Barjat, H. Trace Gas Chemistry in a Young Biomass Burning Plume over Namibia: Observations and Model Simulations: TRACE GAS IN BIOMASS BURNING PLUME OVER NAMIBIA. *J. Geophys. Res.* **2003**, *108*, No. 8482.
(42) Trentmann, J.; Andreae, M. O.; Graf, H. Chemical Processes in a Young Biomass-burning Plume. *J. Geophys. Res.* **2003**, *108*, No. 4705.
(43) Trentmann, J. An Analysis of the Chemical Processes in the Smoke Plume from a Savanna Fire. *J. Geophys. Res.* **2005**, *110*, No. D12301.
(44) Müller, M.; Anderson, B. E.; Beyersdorf, A. J.; Crawford, J. H.; Diskin, G. S.; Eichler, P.; Fried, A.; Keutsch, F. N.; Mikoviny, T.; Thornhill, K. L.; Walega, J. G.; Weinheimer, A. J.; Yang, M.; Yokelson, R. J.; Wisthaler, A. In Situ Measurements and Modeling of Reactive Trace Gases in a Small Biomass Burning Plume. *Atmos. Chem. Phys.* **2016**, *16*, 3813−3824.
(45) Liu, X.; Zhang, Y.; Huey, L. G.; Yokelson, R. J.; Wang, Y.; Jimenez, J. L.; Campuzano-Jost, P.; Beyersdorf, A. J.; Blake, D. R.; Choi, Y.; St Clair, J. M.; Crounse, J. D.; Day, D. A.; Diskin, G. S.; Fried, A.; Hall, S. R.; Hanisco, T. F.; King, L. E.; Meinardi, S.; Mikoviny, T.; Palm, B. B.; Peischl, J.; Perring, A. E.; Pollack, I. B.; Ryerson, T. B.; Sachse, G.; Schwarz, J. P.; Simpson, I. J.; Tanner, D. J.; Thornhill, K. L.; Ullmann, K.; Weber, R. J.; Wennberg, P. O.; Wisthaler, A.; Wolfe, G. M.; Ziemba, L. D. Agricultural Fires in the Southeastern U.S. during $SEAC^4RS$: Emissions of Trace Gases and Particles and Evolution of Ozone, Reactive Nitrogen, and Organic Aerosol: Agricultural Fires in the SE US. *J. Geophys. Res.* **2016**, *121*, 7383−7414.
(46) Peng, Q.; Palm, B. B.; Melander, K. E.; Lee, B. H.; Hall, S. R.; Ullmann, K.; Campos, T.; Weinheimer, A. J.; Apel, E. C.; Hornbrook, R. S.; Hills, A. J.; Montzka, D. D.; Flocke, F.; Hu, L.; Permar, W.; Wielgasz, C.; Lindaas, J.; Pollack, I. B.; Fischer, E. V.; Bertram, T. H.; Thornton, J. A. HONO Emissions from Western U.S. Wildfires Provide Dominant Radical Source in Fresh Wildfire Smoke. *Environ. Sci. Technol.* **2020**, *54*, 5954−5963.
(47) Sparks, T. L.; Ebben, C. J.; Wooldridge, P. J.; Lopez-Hilfiker, F. D.; Lee, B. H.; Thornton, J. A.; McDuffie, E. E.; Fibiger, D. L.; Brown, S. S.; Montzka, D. D.; Weinheimer, A. J.; Schroder, J. C.; Campuzano-Jost, P.; Jimenez, J. L.; Cohen, R. C. Comparison of Airborne Reactive Nitrogen Measurements During WINTER. *J. Geophys. Res.* **2019**, *124*, 10483−10502.
(48) Juncosa Calahorrano, J. F.; Lindaas, J.; O'Dell, K.; Palm, B. B.; Peng, Q.; Flocke, F.; Pollack, I. B.; Garofalo, L. A.; Farmer, D. K.; Pierce, J. R.; Collett, J. L.; Weinheimer, A.; Campos, T.; Hornbrook, R. S.; Hall, S. R.; Ullmann, K.; Pothier, M. A.; Apel, E. C.; Permar, W.; Hu, L.; Hills, A. J.; Montzka, D.; Tyndall, G.; Thornton, J. A.; Fischer, E. V. Daytime Oxidized Reactive Nitrogen Partitioning in Western U.S. Wildfire Smoke Plumes. *J. Geophys. Res.* **2021**, *126* e2020JD033484. DOI: 10.1029/2020JD033484.

https://doi.org/10.1021/acs.est.1c01963
Environ. Sci. Technol. XXXX, XXX, XXX−XXX

(49) Crosson, E. R. A Cavity Ring-down Analyzer for Measuring Atmospheric Levels of Methane, Carbon Dioxide, and Water Vapor. *Appl. Phys. B* **2008**, *92*, 403−408.
(50) Mondello, L.; Tranchida, P. Q.; Dugo, P.; Dugo, G. Comprehensive Two-Dimensional Gas Chromatography-Mass Spectrometry: A Review. *Mass Spectrom. Rev.* **2008**, *27*, 101−124.
(51) Hatch, L. E.; Luo, W.; Pankow, J. F.; Yokelson, R. J.; Stockwell, C. E.; Barsanti, K. C. Identification and Quantification of Gaseous Organic Compounds Emitted from Biomass Burning Using Two-Dimensional Gas Chromatography−Time-of-Flight Mass Spectrometry. *Atmos. Chem. Phys.* **2015**, *15*, 1865−1899.
(52) Lee, B. H.; Lopez-Hilfiker, F. D.; Mohr, C.; Kurtén, T.; Worsnop, D. R.; Thornton, J. A. An Iodide-Adduct High-Resolution Time-of-Flight Chemical-Ionization Mass Spectrometer: Application to Atmospheric Inorganic and Organic Compounds. *Environ. Sci. Technol.* **2014**, *48*, 6309−6317.
(53) Palm, B. B.; Liu, X.; Jimenez, J. L.; Thornton, J. A. Performance of a New Coaxial Ion−Molecule Reaction Region for Low-Pressure Chemical Ionization Mass Spectrometry with Reduced Instrument Wall Interactions. *Atmos. Meas. Tech.* **2019**, *12*, 5829−5844.
(54) DeCarlo, P. F.; Kimmel, J. R.; Trimborn, A.; Northway, M. J.; Jayne, J. T.; Aiken, A. C.; Gonin, M.; Fuhrer, K.; Horvath, T.; Docherty, K. S.; Worsnop, D. R.; Jimenez, J. L. Field-Deployable, High-Resolution, Time-of-Flight Aerosol Mass Spectrometer. *Anal. Chem.* **2006**, *78*, 8281−8289.
(55) Liggio, J.; Li, S.-M.; Hayden, K.; Taha, Y. M.; Stroud, C.; Darlington, A.; Drollette, B. D.; Gordon, M.; Lee, P.; Liu, P.; Leithead, A.; Moussa, S. G.; Wang, D.; O'Brien, J.; Mittermeier, R. L.; Brook, J. R.; Lu, G.; Staebler, R. M.; Han, Y.; Tokarek, T. W.; Osthoff, H. D.; Makar, P. A.; Zhang, J.; L Plata, D.; Gentner, D. R. Oil Sands Operations as a Large Source of Secondary Organic Aerosols. *Nature* **2016**, *534*, 91−94.
(56) Fry, J. L.; Brown, S. S.; Middlebrook, A. M.; Edwards, P. M.; Campuzano-Jost, P.; Day, D. A.; Jimenez, J. L.; Allen, H. M.; Ryerson, T. B.; Pollack, I.; Graus, M.; Warneke, C.; de Gouw, J. A.; Brock, C. A.; Gilman, J.; Lerner, B. M.; Dubé, W. P.; Liao, J.; Welti, A. Secondary Organic Aerosol (SOA) Yields from NO_3 Radical + Isoprene Based on Nighttime Aircraft Power Plant Plume Transects. *Atmos. Chem. Phys.* **2018**, *18*, 11663−11682.
(57) Warneke, C.; Trainer, M.; de Gouw, J. A.; Parrish, D. D.; Fahey, D. W.; Ravishankara, A. R.; Middlebrook, A. M.; Brock, C. A.; Roberts, J. M.; Brown, S. S.; Neuman, J. A.; Lerner, B. M.; Lack, D.; Law, D.; Hübler, G.; Pollack, I.; Sjostedt, S.; Ryerson, T. B.; Gilman, J. B.; Liao, J.; Holloway, J.; Peischl, J.; Nowak, J. B.; Aikin, K. C.; Min, K.-E.; Washenfelder, R. A.; Graus, M. G.; Richardson, M.; Markovic, M. Z.; Wagner, N. L.; Welti, A.; Veres, P. R.; Edwards, P.; Schwarz, J. P.; Gordon, T.; Dube, W. P.; McKeen, S. A.; Brioude, J.; Ahmadov, R.; Bougiatioti, A.; Lin, J. J.; Nenes, A.; Wolfe, G. M.; Hanisco, T. F.; Lee, B. H.; Lopez-Hilfiker, F. D.; Thornton, J. A.; Keutsch, F. N.; Kaiser, J.; Mao, J.; Hatch, C. D. Instrumentation and Measurement Strategy for the NOAA SENEX Aircraftcampaign as Part of the Southeast Atmosphere Study 2013. *Atmos. Meas. Tech.* **2016**, *9*, 3063−3093.
(58) Holmes, C. D.; Fite, C.; Agastra, A.; Schwarz, J. P.; Yokelson, R. J.; Bui, T. V.; Peterson, D. A. In *Critical Evaluation of Smoke Age Inferred from Different Methods During FIREX-AQ*, AGU Fall Meeting, 2020.
(59) Wolfe, G. M.; Marvin, M. R.; Roberts, S. J.; Travis, K. R.; Liao, J. The Framework for 0-D Atmospheric Modeling (F0AM) v3.1. *Geosci. Model Dev.* **2016**, *9*, 3309−3319.
(60) Wagner, N. L.; Riedel, T. P.; Young, C. J.; Bahreini, R.; Brock, C. A.; Dubé, W. P.; Kim, S.; Middlebrook, A. M.; Öztürk, F.; Roberts, J. M.; Russo, R.; Sive, B.; Swarthout, R.; Thornton, J. A.; VandenBoer, T. C.; Zhou, Y.; Brown, S. S. N_2O_5 Uptake Coefficients and Nocturnal NO_2 Removal Rates Determined from Ambient Wintertime Measurements: WINTERTIME N_2O_5 UPTAKE COEFFICIENTS. *J. Geophys. Res.* **2013**, *118*, 9331−9350.
(61) McDuffie, E. E.; Fibiger, D. L.; Dubé, W. P.; Lopez-Hilfiker, F.; Lee, B. H.; Thornton, J. A.; Shah, V.; Jaeglé, L.; Guo, H.; Weber, R. J.; Michael Reeves, J.; Weinheimer, A. J.; Schroder, J. C.; Campuzano-Jost, P.; Jimenez, J. L.; Dibb, J. E.; Veres, P.; Ebben, C.; Sparks, T. L.; Wooldridge, P. J.; Cohen, R. C.; Hornbrook, R. S.; Apel, E. C.; Campos, T.; Hall, S. R.; Ullmann, K.; Brown, S. S. Heterogeneous N_2O_5 Uptake During Winter: Aircraft Measurements During the 2015 WINTER Campaign and Critical Evaluation of Current Parameterizations. *J. Geophys. Res.* **2018**, *123*, 4345−4372.
(62) Decker, Z. C. J.; Zarzana, K. J.; Coggon, M.; Min, K.-E.; Pollack, I.; Ryerson, T. B.; Peischl, J.; Edwards, P.; Dubé, W. P.; Markovic, M. Z.; Roberts, J. M.; Veres, P. R.; Graus, M.; Warneke, C.; de Gouw, J.; Hatch, L. E.; Barsanti, K. C.; Brown, S. S. Nighttime Chemical Transformation in Biomass Burning Plumes: A Box Model Analysis Initialized with Aircraft Observations. *Environ. Sci. Technol.* **2019**, *53*, 2529−2538.
(63) Finewax, Z.; de Gouw, J. A.; Ziemann, P. J. Identification and Quantification of 4-Nitrocatechol Formed from OH and NO_3 Radical-Initiated Reactions of Catechol in Air in the Presence of NO_x: Implications for Secondary Organic Aerosol Formation from Biomass Burning. *Environ. Sci. Technol.* **2018**, *52*, 1981−1989.
(64) Schwantes, R. H.; Schilling, K. A.; McVay, R. C.; Lignell, H.; Coggon, M. M.; Zhang, X.; Wennberg, P. O.; Seinfeld, J. H. Formation of Highly Oxygenated Low-Volatility Products from Cresol Oxidation. *Atmos. Chem. Phys.* **2017**, *17*, 3453−3474.
(65) Jenkin, M. E.; Saunders, S. M.; Pilling, M. J. The Tropospheric Degradation of Volatile Organic Compounds: A Protocol for Mechanism Development. *Atmos. Environ.* **1997**, *31*, 81−104.
(66) Saunders, S. M.; Jenkin, M. E.; Derwent, R. G.; Pilling, M. J. Protocol for the development of the Master Chemical Mechanism, MCM v3 (Part A): tropospheric degradation of non-aromatic volatile organic compounds. *Atmos. Chem. Phys.* **2003**, *3*, 161−180.
(67) Permar, W.; Wang, Q.; Selimovic, V.; Wielgasz, C.; Yokelson, R. J.; Hornbrook, R. S.; Hills, A. J.; Apel, E. C.; Ku, I.; Zhou, Y.; Sive, B. C.; Sullivan, A. P.; Collett, J. L.; Campos, T. L.; Palm, B. B.; Peng, Q.; Thornton, J. A.; Garofalo, L. A.; Farmer, D. K.; Kreidenweis, S. M.; Levin, E. J. T.; DeMott, P. J.; Flocke, F.; Fischer, E. V.; Hu, L. Emissions of Trace Organic Gases from Western U.S. Wildfires Based on WE-CAN Aircraft Measurements. *J. Geophys. Res.* **2021**, *126* (11), e2020JD033838 DOI: 10.1029/2020JD033838.
(68) Sekimoto, K.; Koss, A. R.; Gilman, J. B.; Selimovic, V.; Coggon, M. M.; Zarzana, K. J.; Yuan, B.; Lerner, B. M.; Brown, S. S.; Warneke, C.; Yokelson, R. J.; Roberts, J. M.; de Gouw, J. High- and Low-Temperature Pyrolysis Profiles Describe Volatile Organic Compound Emissions from Western US Wildfire Fuels. *Atmos. Chem. Phys.* **2018**, *18*, 9263−9281.
(69) Yokelson, R. J.; Griffith, D. W. T.; Ward, D. E. Open-Path Fourier Transform Infrared Studies of Large-Scale Laboratory Biomass Fires. *J. Geophys. Res.* **1996**, *101*, 21067−21080.
(70) Selimovic, V.; Yokelson, R. J.; Warneke, C.; Roberts, J. M.; de Gouw, J.; Reardon, J.; Griffith, D. W. T. Aerosol Optical Properties and Trace Gas Emissions by PAX and OP-FTIR for Laboratory-Simulated Western US Wildfires during FIREX. *Atmos. Chem. Phys.* **2018**, *18*, 2929−2948.
(71) Yokelson, R. J.; Andreae, M. O.; Akagi, S. K. Pitfalls with the Use of Enhancement Ratios or Normalized Excess Mixing Ratios Measured in Plumes to Characterize Pollution Sources and Aging. *Atmos. Meas. Tech.* **2013**, *6*, 2155−2158.
(72) Sommariva, R.; Brown, S. S.; Roberts, J. M.; Brookes, D. M.; Parker, A. E.; Monks, P. S.; Bates, T. S.; Bon, D.; de Gouw, J. A.; Frost, G. J.; Gilman, J. B.; Goldan, P. D.; Herndon, S. C.; Kuster, W. C.; Lerner, B. M.; Osthoff, H. D.; Tucker, S. C.; Warneke, C.; Williams, E. J.; Zahniser, M. S. Ozone Production in Remote Oceanic and Industrial Areas Derived from Ship Based Measurements of Peroxy Radicals during TexAQS 2006. *Atmos. Chem. Phys.* **2011**, *11*, 2471−2485.
(73) Cazorla, M.; Brune, W. H.; Ren, X.; Lefer, B. Direct Measurement of Ozone Production Rates in Houston in 2009 and Comparison with Two Estimation Methods. *Atmos. Chem. Phys.* **2012**, *12*, 1203−1212.

https://doi.org/10.1021/acs.est.1c01963
Environ. Sci. Technol. XXXX, XXX, XXX−XXX

(74) Brune, W. H.; Baier, B. C.; Thomas, J.; Ren, X.; Cohen, R. C.; Pusede, S. E.; Browne, E. C.; Goldstein, A. H.; Gentner, D. R.; Keutsch, F. N.; Thornton, J. A.; Harrold, S.; Lopez-Hilfiker, F. D.; Wennberg, P. O. Ozone Production Chemistry in the Presence of Urban Plumes. *Faraday Discuss.* **2016**, *189*, 169−189.
(75) Baier, B. C.; Brune, W. H.; Miller, D. O.; Blake, D.; Long, R.; Wisthaler, A.; Cantrell, C.; Fried, A.; Heikes, B.; Brown, S.; McDuffie, E.; Flocke, F.; Apel, E.; Kaser, L.; Weinheimer, A. Higher Measured than Modeled Ozone Production at Increased NO_X Levels in the Colorado Front Range. *Atmos. Chem. Phys.* **2017**, *17*, 11273−11292.
(76) Womack, C. C.; McDuffie, E. E.; Edwards, P. M.; Bares, R.; Gouw, J. A.; Docherty, K. S.; Dubé, W. P.; Fibiger, D. L.; Franchin, A.; Gilman, J. B.; Goldberger, L.; Lee, B. H.; Lin, J. C.; Long, R.; Middlebrook, A. M.; Millet, D. B.; Moravek, A.; Murphy, J. G.; Quinn, P. K.; Riedel, T. P.; Roberts, J. M.; Thornton, J. A.; Valin, L. C.; Veres, P. R.; Whitehill, A. R.; Wild, R. J.; Warneke, C.; Yuan, B.; Baasandorj, M.; Brown, S. S. An Odd Oxygen Framework for Wintertime Ammonium Nitrate Aerosol Pollution in Urban Areas: NO_x and VOC Control as Mitigation Strategies. *Geophys. Res. Lett.* **2019**, *46*, 4971−4979.
(77) McDuffie, E. E.; Edwards, P. M.; Gilman, J. B.; Lerner, B. M.; Dubé, W. P.; Trainer, M.; Wolfe, D. E.; Angevine, W. M.; deGouw, J.; Williams, E. J.; Tevlin, A. G.; Murphy, J. G.; Fischer, E. V.; McKeen, S.; Ryerson, T. B.; Peischl, J.; Holloway, J. S.; Aikin, K.; Langford, A. O.; Senff, C. J.; Alvarez, R. J.; Hall, S. R.; Ullmann, K.; Lantz, K. O.; Brown, S. S. Influence of Oil and Gas Emissions on Summertime Ozone in the Colorado Northern Front Range: COLORADO O&G AND SUMMERTIME OZONE. *J. Geophys. Res.* **2016**, *121*, 8712−8729.
(78) Chameides, W.; Lindsay, R.; Richardson, J.; Kiang, C. The Role of Biogenic Hydrocarbons in Urban Photochemical Smog: Atlanta as a Case Study. *Science* **1988**, *241*, 1473−1475.
(79) Levy, H. Normal Atmosphere: Large Radical and Formaldehyde Concentrations Predicted. *Science* **1971**, *173*, 141−143.
(80) Neuman, J. A.; Trainer, M.; Brown, S. S.; Min, K.-E.; Nowak, J. B.; Parrish, D. D.; Peischl, J.; Pollack, I. B.; Roberts, J. M.; Ryerson, T. B.; Veres, P. R. HONO Emission and Production Determined from Airborne Measurements over the Southeast U.S.: HONO OVER THE SOUTHEAST U.S. *J. Geophys. Res.* **2016**, *121*, 9237−9250.
(81) Martinez, M. OH and HO_2 Concentrations, Sources, and Loss Rates during the Southern Oxidants Study in Nashville, Tennessee, Summer 1999. *J. Geophys. Res.* **2003**, *108*, No. 4617.
(82) Harrison, M. A. J.; Barra, S.; Borghesi, D.; Vione, D.; Arsene, C.; Iulian Olariu, R. Nitrated Phenols in the Atmosphere: A Review. *Atmos. Environ.* **2005**, *39*, 231−248.
(83) Chen, J.; Wenger, J. C.; Venables, D. S. Near-Ultraviolet Absorption Cross Sections of Nitrophenols and Their Potential Influence on Tropospheric Oxidation Capacity. *J. Phys. Chem. A* **2011**, *115*, 12235−12242.
(84) Woodill, L. A.; Hinrichs, R. Z. Heterogeneous Reactions of Surface-Adsorbed Catechol with Nitrogen Dioxide: Substrate Effects for Tropospheric Aerosol Surrogates. *Phys. Chem. Chem. Phys.* **2010**, *12*, 10766.
(85) Sakamoto, Y.; Sadanaga, Y.; Li, J.; Matsuoka, K.; Takemura, M.; Fujii, T.; Nakagawa, M.; Kohno, N.; Nakashima, Y.; Sato, K.; Nakayama, T.; Kato, S.; Takami, A.; Yoshino, A.; Murano, K.; Kajii, Y. Relative and Absolute Sensitivity Analysis on Ozone Production in Tsukuba, a City in Japan. *Environ. Sci. Technol.* **2019**, *53*, 13629−13635.
(86) Schroeder, J. R.; Crawford, J. H.; Fried, A.; Walega, J.; Weinheimer, A.; Wisthaler, A.; Müller, M.; Mikoviny, T.; Chen, G.; Shook, M.; Blake, D. R.; Tonnesen, G. S. New Insights into the Column CH_2O/NO_2 Ratio as an Indicator of near-Surface Ozone Sensitivity: CH_2O/NO_2 as Indicator of O_3 Sensitivity. *J. Geophys. Res.* **2017**, *122*, 8885−8907.

https://doi.org/10.1021/acs.est.1c01963
Environ. Sci. Technol. XXXX, XXX, XXX−XXX